Proceedings of the 21st ICSMGE, Vienna, Austria, 14 – 19 June 2026. Pistrol, Adam & Schweiger (eds.)
Published by: ÖGG, Austrian Society for Geomechanics, Salzburg, Austria, ISBN 978-3-9503898-4-5
https://doi.org/10.53243/ICSMGE2026-1412

Ground load assessment on buried flexible pipes subjected to lateral soil movement

Saifa Anzum, Ashutosh Sutra Dhar
Department of Civil Engineering, Memorial University of Newfoundland, St. John's, NL, Canada, saprioty@mun.ca

ABSTRACT: Underground pipeline systems play a critical role in modern society by transporting water, wastewater, and energy. Ground movements due to landslides and seismic activities often pose pipeline hazards. The moving ground can cause excessive strains in the pipe wall, leading to rupture and service disruption. Current design guidelines recommend the "beam-on-spring" analysis to evaluate pipe wall strains due to the ground movements. The recommended spring parameters are based on laboratory tests on steel pipeline segments. The spring forces normalized by the pipe length and diameter were obtained from the tests assuming plane strain condition, ignoring the bending of the pipe segment during the tests. However, pipe wall bending might be significant for flexible pipes, which cannot be overlooked while interpreting test results. The authors' studies have indicated that the length of the pipe segment, pipe diameter, and modulus of elasticity of soil and pipe influence the behavior of pipes in full-scale laboratory tests. Considering these factors, this paper investigates ground loads on buried flexible when subjected to lateral ground movement. Data from full-scale tests conducted with flexible medium-density polyethylene (MDPE) pipe were critically examined. Pipe deflections, wall strains, and ground loads measured in the full-scale tests were examined. Three-dimensional finite element (FE) modeling was employed to investigate the ground loads along the length of the pipes, which could not be measured during the tests. The FE model was developed using commercially available software, ABAQUS, by calibrating it with the test data. The study reveals that the flexural rigidity of the soil-pipe system significantly influences the behavior of the pipe during the tests, which cannot be idealized as a plane strain condition. As a result, the ground force along the length of the pipe was nonuniform. Thus, spring forces recommended in the design guidelines may not be applicable to flexible pipes.

KEYWORDS: Ground movement, flexible pipes, lateral load, full-scale test, numerical analysis.

1 INTRODUCTION

Energy pipelines are often routed, buried, or exposed through various landscapes where natural hazards like seismic activity, recurring landslides, and soil deformation or liquefaction are present. Assessing the structural integrity of these pipes to comply with the environmental regulatory requirements impose challenges on pipeline engineers.

Over the years, pipeline engineers have studied the effect of ground movement on buried pipelines and developed state-of-the-art design guidelines for the analysis and design of the pipelines (ALA 2005, PRCI 2017). The current state of practice addresses the pipeline–landslide interaction in a simplified manner, representing the soil-pipeline system as a structural beam (pipe) interacting with three orthogonal springs (soil). These suggest idealized elastoplastic models for the springs characterized by two parameters: the maximum force and the corresponding maximum elastic deformation. These parameters were formulated based on the measurements obtained from the laboratory tests conducted by Audibert and Nyman (1978), Trautmann and O'Rourke (1985), and numerical results from Yimsiri et al. (2004). The majority of the laboratory tests were performed on rigid pipe segments, representing plane strain conditions. Moreover, the maximum normalized soil resistance from the empirical fits of the test loads was typically based on the burial depth to diameter ratio and surrounding soil properties. Figure 1 shows a comparison of two test results from Audibert and Nyman (1978) and Trautmann and O'Rourke (1985) with those obtained from design guideline recommendations. It shows that ALA (2005) overpredicts the maximum lateral soil forces for both tests by 80% to 150%. Audibert and Nyman (1978) reported good agreement between their tests and the Hansen (1961) model, which was used in ALA (2005). However, ALA (2005) failed to predict the small diameter (25.4-mm diameter) pipe test results from Audibert and Nyman (1978) (Figure 1). On the other hand, PRCI (2017) adopted parameters using the test results from Trautmann and O'Rourke (1985) and numerical results from Yimsiri et al. (2004), which reasonably predicted both the tests. However, it did not successfully identify the peak in one of the tests, as seen in Figure 1. The overall inconsistency in the existing guidelines questions the efficacy of the simplified design recommendations in the guidelines. Besides, the applicability of the design guide recommendations for flexible pipes was not evaluated through measurements.

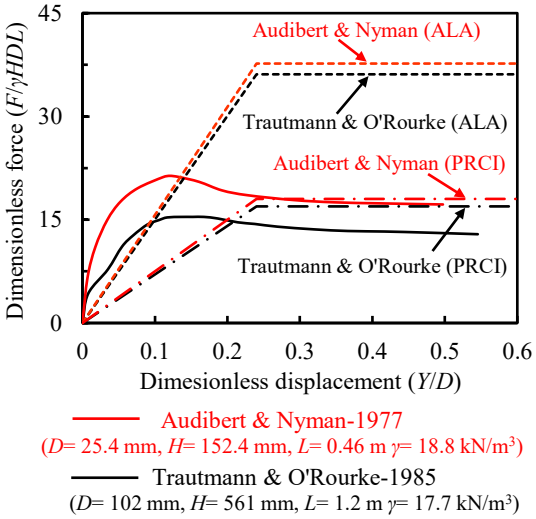

Figure 1. Comparison of normalized pullout forces

Flexible pipelines do not exhibit plane strain behavior when subjected to ground movement, instead, undergo bending and localized ovalization. These make the interpretation of the test results challenging. Xie et al. (2013) experimented on the spring force for a high-density polyethylene (HDPE) pipeline subject to normal faulting and found the maximum force to be one-tenth of the force values of steel pipes. Almahakeri et al. (2017), Liu et al. (2023), and Ye et al. (2025) carried out further experiments on how the flexural rigidity of the soil–pipe system influences the overall behavior under various soil-loading directions. They found that existing guidelines greatly overpredict soil resistance for flexible pipes. Therefore, in-depth analysis on flexible pipes using both laboratory testing

and numerical simulation can provide a better understanding for establishing a design guideline for these pipes.

The purpose of this study is to conduct large-scale laboratory tests and numerical modeling for 60-mm diameter steel and Medium Density Polyethylene (MDPE) pipes subjected to lateral ground movement. The ends of the pipes buried in soil tank were fixed and the tank was moved laterally to simulate a ground movement scenario. The load-displacement responses, pipe strains, and deformations from the experimental work are examined. The response of the soil-pile system from the test was investigated using three-dimensional (3D) finite element modeling. The discussion concludes with an evaluation of how the flexural rigidity of the soil-pipe system affects the horizontal load from ground movement.

2 EXPERIMENTAL SETUP

The testing facility was developed at Memorial University of Newfoundland to simulate ground movement scenario by anchoring the buried pipe outside a moving soil tank (see Figure 2). The setup consists of 4.0 × 2.0 × 1.5 m (L × W × D) reinforced steel soil tank placed on a frame with linear bearings mounted on tracks to slide. One side of the tank is mounted with a frame that connects to the hydraulic RAM for pulling, allowing for movement up to 150 mm. A vertical frame, on the other side of the tank, supports the load cells and potentiometers connected to the pipe and the tank for the measurements of loads and displacements.

The test pipes were measured 1.9 m in length, with a 50 mm space from the tank wall to the pipe end surface to avoid friction during testing. The ends of the steel pipe are capped with plates to keep soil out during the experiments. For MDPE pipes, end plugs made of aluminum were used both to block soil ingress and to prevent wall buckling and resulting slippage of grips. Both ends of the pipes were fixed by steel cables connected to the load cells while allowing vertical movements and rotation. Details of the two tests are summarized in Table 1. Figure 2 shows a typical instrumented MDPE pipe laid on the soil bed. Strain was measured using fiber optic sensors (FO) at both opposite springlines.

Table 1. Test program.

Parameter	Steel pipe test	MDPE pipe test
Burial depth, H (mm)	600	
Pipe diameter, D (mm)	60.3	
Pipe thickness, t (mm)	3.91	5.48
Buried length, L (m)	1.9	
Pull rate (mm/min)	0.5	
Instrumentation	FO	FO + SG
Soil displacement (mm)	120	
Soil condition	Dense	

Additional strain gauges (SG) were placed on the MDPE pipe specifically at locations of high strain as the strain beyond 1.2% could not be measured using the current setup of FO sensor system. Pipe deformation with soil tank displacement was measured using string potentiometers. Figure 2 presents the essential details of the test program. For the backfill material, locally manufactured well-graded sand was used during testing. The soil was compacted using a vibratory plate tamper to obtain approximately the density of 18 kN/m^3 at around 95% of standard Proctor relative compaction.

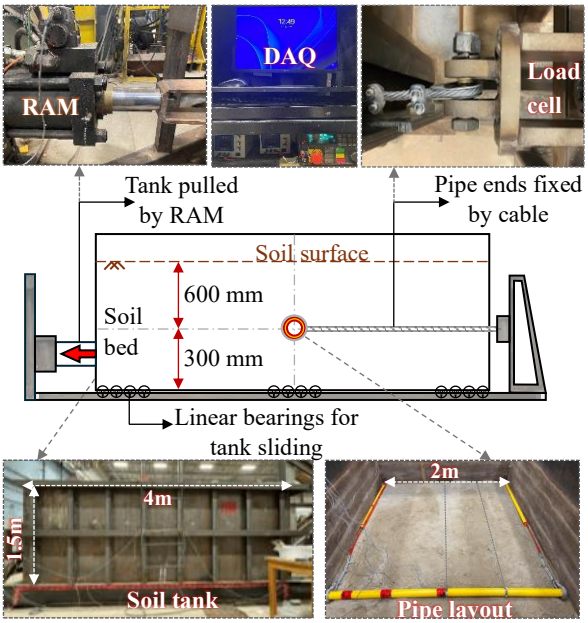

Figure 2. Testing facility for lateral pullout test

3 PIPE–SOIL RESPONSES FROM TESTS

Figure 3 presents the load–soil displacement response for two types of buried pipes: a steel pipe and a Medium-Density Polyethylene (MDPE) pipe, both with an outer diameter (D) of 60 mm and an embedment height (H) of 600 mm. The soil tank was pulled up to 120 mm perpendicular to the pipe axis. The test results are compared with predictions using the ALA (2005) and PRCI (2017) models. Given that the current soil-pipe interaction scenario includes bending and reflects a three-dimensional condition rather than a plane strain case, the comparison is made using the total pullout load instead of the dimensionless lateral soil resistance, N_{qh} ($F/\gamma HDL$), where γ is effective unit weight of soil and F is total force applied to the pipeline and L is the pipe length.

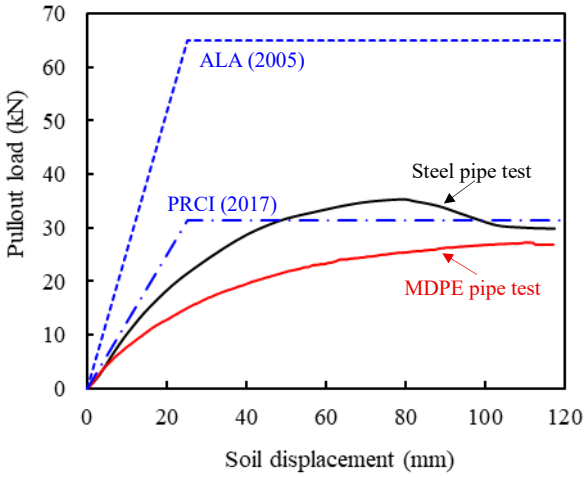

Figure 3. Force–displacement curves for lateral soil pullout tests

The results indicate a difference in load-displacement responses between the two pipe materials. The steel pipe response demonstrates a peak load of approximately 35 kN at around 70 mm of soil displacement, followed by a gradual reduction in load, suggesting a post-peak softening behavior possibly due to local soil failure or interface degradation. In contrast, the MDPE pipe displays a more ductile response, with

the load increasing steadily and plateauing near 26 kN. This suggests that the MDPE pipe deforms progressively, showing lower peak force. The ALA (2005) model significantly overestimates the load for both pipes, particularly more for the MDPE pipe. PRCI (2017) predicts the post peak residual load for the steel pipe reasonably. For the MDPE pipe, the PRCI model slightly overpredicts the peak force, highlighting its limitations in addressing pipe-soil flexibility and material effects.

Figure 4 presents the variation of longitudinal strain along the pipe length at a particular soil displacement of 80 mm. In this study, only the longitudinal strain profiles at the passive earth pressure side springline, which is facing the soil load, are presented for both pipes. The tensile strain is indicated by positive values, and compressive strain by negative ones. Figure 4 shows that for a same amount of soil displacement, strain distribution of MDPE pipe significantly differs from steel pipe.

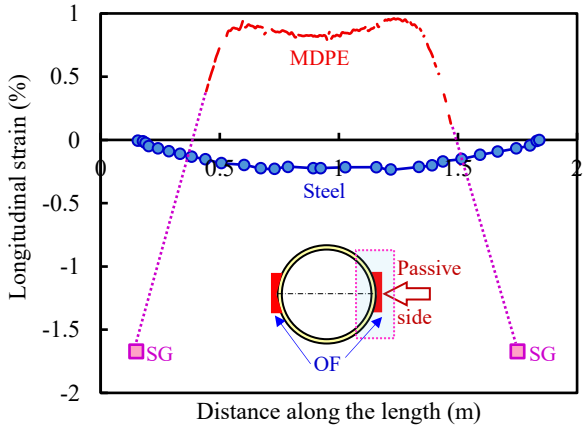

Figure 4. Distributions of bending strains along pipe

As the steel pipe bends due to soil pressure, the springline at the passive side faces compression and the strain maximizes (0.23%) at the midspan. For MDPE pipe, the maximum strain (1.67%) is near the restrained pipe ends, i.e., the interface between the moving and stationary soil. The midspan of this pipe experiences tensile strain nearly 1%, indicating axial stretching during lateral ground load. The results of these analyses demonstrate that, due to the small pipe diameter and the flexibility of the MDPE pipe, the pipe deformation was dominated by both membrane (axial extension) and bending. The fiber optic sensors at the midspan reached its capacity beyond 80-mm soil displacement. And so, the strain data for maximum bending induced compression stresses are unavailable for higher soil displacement. However, the strain of 60-mm MDPE pipe at 80-mm lateral soil displacement (1.68%) was less than the allowable strain limit of 8% for MDPE material (Jana, 2012).

The MDPE pipe movement near mid-span was almost same as the soil displacement (not reported here). Whereas the movement of steel pipe was very minimal compared to the soil displacement. This is because the flexural stiffness of the former pipe is lower than that of the latter which affected the load-deformation behavior. For the highly flexible pipe, most of the pipe portion moves with the soil, leaving a small zone near the ends causing plastic deformation of soil. This could be a reason for no post peak softening of load for MDPE pipe in Figure 3. The test results indicate that it is necessary to consider pipe material and flexibility in assessing ground loads. The current design guidelines may not accurately represent the forces under lateral soil movement, particularly for flexible systems. To understand more about the behavior of flexible pipe under ground load, numerical analysis was performed as presented in the next section.

4 THREE-DIMENSIONAL FINITE ELEMENT ANALYSIS

4.1 *Description of numerical model*

This study adopted Abaqus/Explicit (Dassault Systems, 2019) finite element package for three-dimensional modeling of the pipe tests. A 4 m long block with 1.2 m of height, and 2 m width of soil was modeled, as in the tests. The pipe is placed in the middle of the soil block at a depth of 0.6 m, and it has 2 m of soil on the passive side. The soil is modeled using linear eight-node brick with reduced integration (C3D8R) elements and hour-glassing control. The bottom soil boundary and the other faces are restrained to their perpendicular direction with the displacement degrees of freedom, except for the top of the soil. The appropriate mesh size for the soil is chosen by a sensitivity analysis considering numerical accuracy and efficiency (Anzum & Dhar, 2023). The zone near the pipe is meshed with finer-sized elements, spanning up to 3.5 times the pipe diameter (3.5*D*) from the pipe surface, shown in Figure 5a. For this study, both the steel and MDPE pipes are modeled using shell elements (S4R). Ends of the pipes are restrained at the horizontal direction (marked in red) and allowed to move vertically. The soil and pipe are meshed using the structured meshing approach.

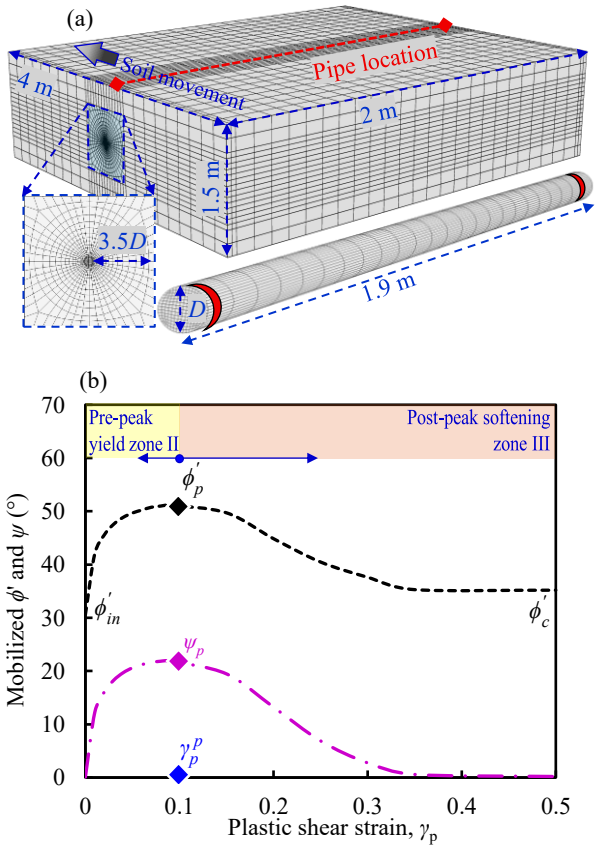

Figure 5. FE model: (a) soil and pipe mesh, (b)Variations of mobilized friction and dilation angle

The interface between pipe and soil is simulated using the general contact surface approach, allowing sliding and separating between the contact surfaces. In this method, the friction coefficient is defined as $\mu = \tan(\delta)$, where $\delta\ (=f\phi_p^{'})$ is the pipe-soil interface friction angle. The interface friction angle is found by reducing the peak friction angle of the soil $\phi_p^{'}$, by a factor *f,* which depends on the pipe surface property. This interface friction factor, *f* is used as 0.8 and 0.6, respectively for rough steel and MDPE pipe, as suggested in ALA (2005) and PRCI (2017).

The analysis is conducted in two steps: geostatic and lateral movement. The geostatic step ensures the initial stress state under $K_0 = 1.0$, where K_0 is the at-rest earth pressure coefficient. A lateral earth pressure coefficient of 1, instead of $\frac{v_{soil}}{1-v_{soil}}$, provides an isotropic initial stress field, which minimizes the shear deformations in the soil, significantly reducing computational time during analysis. However, analyses were performed with the lateral earth pressure coefficient by $\frac{v_{soil}}{1-v_{soil}}$ and were not found to significantly affect the lateral pulling force (the difference was less than 3%). In the second step, the soil is laterally moved by using the displacement boundary condition at all outer surfaces of the soil block except the top. The soil was displaced by 120-mm (perpendicular to the pipe axis). Adaptive meshing using ALE (Arbitrary Lagrangian-Eulerian) is applied to account for the large deformation expected in the soil.

4.1 *Soil Constitutive Model*

Lateral soil movements are commonly simulated using the conventional Mohr-Coulomb model to define soil plasticity, where the internal friction angle ϕ' and dilation angle ψ are considered as constants. However, the behavior of dense sand is state-dependent and influenced by factors such as density, confining pressure, and strain. Therefore, studies are focusing on using more advanced constitutive models to describe the lateral soil-pipe interaction in dense sand (Roy et. al., 2015; Yang et al. 2024.). In this study, soil plasticity is modeled using the Modified Mohr-Coulomb model (MMC), accounting for post-peak strain softening. The mobilized effective peak friction angle ($\phi^{'}$) and dilation angle (ψ) are updated with accumulated equivalent plastic strains and corresponding confining stress shown in Figure 5b. As Abaqus does not include the proposed MMC model, it is implemented by developing a user subroutine (VUSDFLD) written in FORTRAN. Summary of the constitutive relationships of the MMC model and the soil parameters used in the current study are presented in Table 2 and 3, respectively. The details and key features of the MMC model are discussed in Anzum and Dhar (2023). The constitutive model has been calibrated and validated against the numerical data from Roy et al. (2015) for a 150 mm-diameter pipe at 900 mm burial depth (Anzum and Dhar, 2024). For comparison, the tests in this study are modeled using the Mohr-Coulomb model as well.

The Young's modulus (E_s) of soil was determined using Janbu's stress-dependent nonlinear model. Janbu (1963) presented a power function of the confining pressure, $\sigma_c^{'}$, defining the variation of the initial tangent modulus of elasticity, E_s, as shown in Equation (1).

$$E_s = K\,p_A\left(\frac{\sigma_c^{'}}{p_A}\right)^n \quad (1)$$

where n and K = soil-specific Janbu model parameters, $\sigma_c^{'}$ = the mean effective confining pressure = $K_0\gamma H$ and K_0 = the coefficient of lateral earth pressure at rest.

Table 2. Constitutive formulations of the MMC model

Description	Constitutive Equation
Relative density index	$I_R = I_D\left(Q - ln\frac{100\,\sigma_m^{'}}{p_A}\right) - R$, $Q = 7.4 + 0.60\,ln\,\sigma_c^{'}$
Peak friction angle	$\phi_p^{'} = \phi_c^{'} + A_\psi\,I_R$, A_ψ=3.8
Peak dilation angle	$\psi_p = \left(\phi_p^{'} - \phi_c^{'}\right)/k_\psi$, k_ψ=0.5
Strain softening parameter	$\gamma_c^p = C_1 - C_2 I_D$
Plastic strain at $\phi_p^{'}$	$\gamma_p^p = \gamma_c^p\left(\frac{\sigma_m^{'}}{p_A}\right)^m$,
Mobilized friction angle-zone II	$\phi^{'} = \phi_{in}^{'} + \sin^{-1}\left(\frac{2\sqrt{\gamma_p\gamma_p^p}}{\gamma_p + \gamma_p^p}\right)\sin\left(\phi_p^{'} - \phi_{in}^{'}\right)$
Mobilized dilation angle-zone II	$\psi = \sin^{-1}\left(\frac{2\sqrt{\gamma_p\gamma_p^p}}{\gamma_p + \gamma_p^p}\right)\sin\left(\psi_p\right)$
Mobilized friction angle-zone III	$\phi^{'} = \phi_c^{'} + \left(\phi_p^{'} - \phi_c^{'}\right)\exp\left\{-\left(\frac{\gamma_p - \gamma_p^p}{\gamma_c^p}\right)^2\right\}$
Mobilized dilation angle-zone III	$\psi = \psi_p\exp\left\{-\left(\frac{\gamma_p - \gamma_p^p}{\gamma_c^p}\right)^2\right\}$

Note: A_ψ slope of $\left(\phi_p^{'} - \phi_c^{'}\right)$ versus I_R; m, C_1, C_2 = soil parameters; I_R= relative density index; k_ψ slope of $\left(\phi_p^{'} - \phi_c^{'}\right)$ versus ψ_p; $\phi_{in}^{'}$ = at the start of plastic deformation; $\phi_p^{'}$= peak friction angle; $\phi_c^{'}$= critical state friction angle; ψ_p= peak dilation angle; γ_p= plastic shear strain; γ_p^p= γ_p required to mobilize $\phi_p^{'}$; γ_c^p= strain softening parameter.

4.2 *Pipe Constitutive Model*

For the steel pipe material, an elastoplastic response for the steel is modeled using the isotropic Von Mises plasticity model available in ABAQUS. The stress–strain relation of steel has been adapted from Almahakeri et al. (2018).

Table 3. Summary of input parameters for soil and pipe material

Material	Parameter	Value
Soil	Poisson's ratio, v_{soil}	0.3
	Critical-state friction angle, $\phi_c^{'}$ (°)	35
	Relative density, I_D (%)	85
	Unit weight, γ (kN/m^3)	18
	Interface friction coefficient, μ	tan(0.8ϕ')
	Cohesion, c' (kN/m^2) [a]	0.1
	C_1	0.22
	C_2	0.11
	m	0.25
	K	150
	n	0.5
	p_A(kN/m^2)	100
Steel pipe	Modulus of elasticity (GPa)	210
	Poisson's ratio, v	0.33
	Density (kg/m^3)	7800
MDPE pipe	Initial modulus of elasticity (MPa)	515
	Poisson's ratio, v	0.46
	Density (kg/m^3)	940

In the case of MDPE pipe material, the strain rate-dependent hyperbolic model was developed, according to Suleiman and Coree (2004), assuming isotropic elastic-plastic behavior. Details of the MDPE pipe property definition are discussed in Anzum and Dhar (2023). The parameters required for modeling steel and MDPE pipes are listed in Table 3.

5 RESULTS AND DISCUSSION

5.1 *Simulation of responses*

The comparison of the force–displacement responses from FE simulations and experiments is shown in Figure 6. It reveals that for the steel pipe buried in dense sand, the MMC model captures the peak load and strain-softening behavior better, while the MC model tends to overestimate post-peak forces. For MDPE pipes, the MC and MMC models yield almost identical responses and replicate the experimental results very well. The similarity between the results from two models for MDPE pipe behavior is likely due to the pipe's flexible nature, resulting in less soil plastic deformation, making it less sensitive to the post-peak plastic deformation.

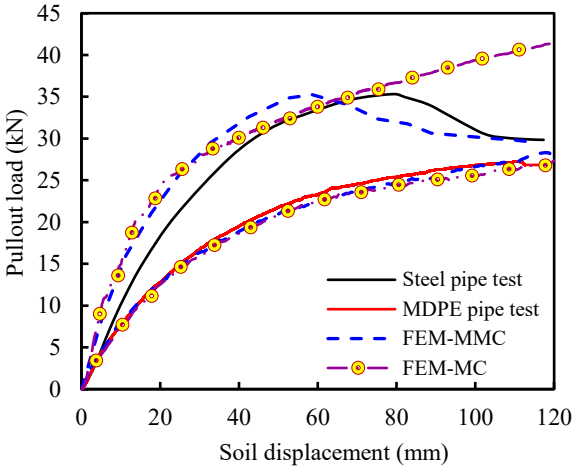

Figure 6. Numerical model fitting against experimental load–displacement data

Figure 7a and 7b present the longitudinal strain measured 150 mm away from the pipe ends at two opposing springlines for MDPE pipe. Strain gauges (SG) were used to record these strains at locations experiencing the maximum soil deformation, which resulted in higher pipe strain.

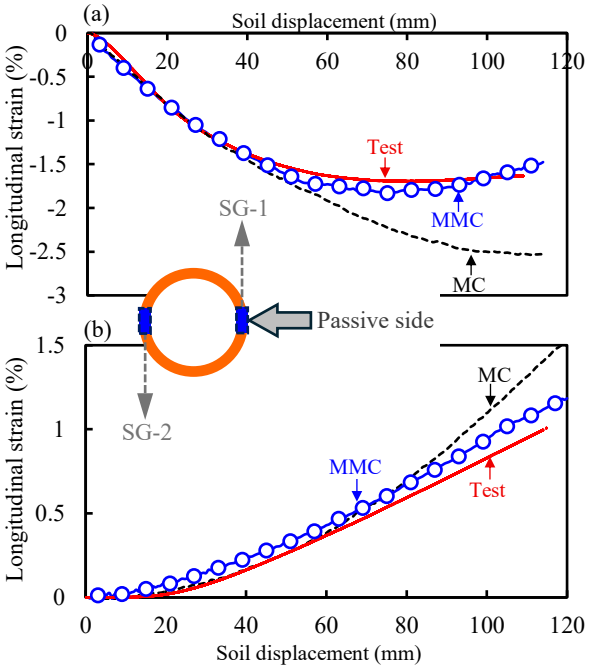

Figure 7. Test strain simulation: (a) Passive side strain, (b) active side strain

The passive side strain gauge, SG-1, measured the compressive strain that increases with tank displacement of up to 80 mm and then decreases slowly to almost a constant value (Figure 7a). This reduction in strain is captured by the MMC model, while the MC model, having the same initial slope, continues to increase with soil displacement. Note that although the MC model reasonably simulates the load–displacement response (Figure 6), the MMC model better predicted the localized response (i.e., strain), indicating localized post-peak degradation of the friction angle. As the plastic deformation of soil did not extend too far along the pipe length, the global response (i.e., load–displacement) was not affected.

Figure 7b shows that for SG-2, there was no reduction in tensile strain, and both MMC and MC model followed the same trend with the test results. However, the MC model predicted higher strain after 80 mm of tank displacement. Therefore, although the overall soil–pipe response does not show any softening response due to a small zone of plastically deformed soil for MDPE pipe, the MMC better simulates the pipe-soil interaction for both pipes.

5.2 *Soil-pipe Interaction force*

As the FE model with MMC simulated the test results better, the results of the FE analysis were used to examine the maximum lateral soil force for the steel and MDPE pipes. Figure 8 shows the contact pressure distribution around the pipe circumference from the 3D analysis at 150-mm from the pipe end for both pipes. Only the data for 120-mm tank displacement is presented. The stress is distributed around the springline at the passive side of the soil and extends near the shoulder and haunches of the steel pipe. For the MDPE pipe, the magnitude of the stress is close to the steel pipe, but it is less distributed around the circumference. At the springline, there is a reduction in stress. The ovalization of the flexible pipe might create a void between the pipe surface and soil, resulting in low contact pressure.

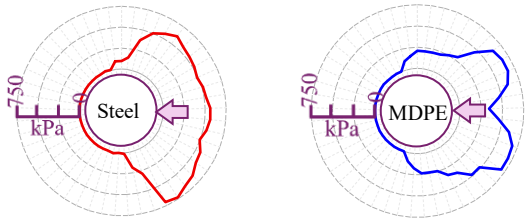

Figure 8. Contact pressure distributions at 120 mm tank displacement

The contact pressure distribution can be integrated to obtain the lateral force by the method adopted by Choo et. al. (2007) and O'Rourke et al. (2016). As shown in Figure 9a, the normal pressure, P_m, and the tangential pressure, acting over an arc length, can be resolved to obtain the horizontal components. Taking the horizontal component of normal and tangential pressure, and integrating around the circumference, the lateral force per unit length of pipe, P_h, is determined, as given in Equation (2).

$$P_h = \int_0^{2\pi} P_m S_\theta \sin\theta \, d\theta + \int_0^{2\pi} \mu P_m S_\theta \cos\theta \, d\theta \qquad (2)$$

Herein, P_m is the contact normal pressure, S_θ is the arc length having pressure, θ is the angle for the orientation of P_m. From the horizontal soil force per meter length of the pipe, the N_{qh} is calculated at the 150-mm section from the pipe end, where the maximum soil force was mobilized. The calculated N_{qh} is compared with those from ALA (2005) and PRCI (2017) design

guidelines in Figure 9b. The results are presented against the relative soil pipe stiffness, E_p/E_s, similar to Saiyar et. al. (2016). Here, E_p, E_s are the elastic modulus for pipe and soil, respectively. Figure 9b. shows that the steel pipe, with significantly higher stiffness, shows a much larger dimensionless soil force, N_{qh}, compared to the flexible MDPE pipe, reflecting the influence of flexural rigidity on the soil force mobilization.

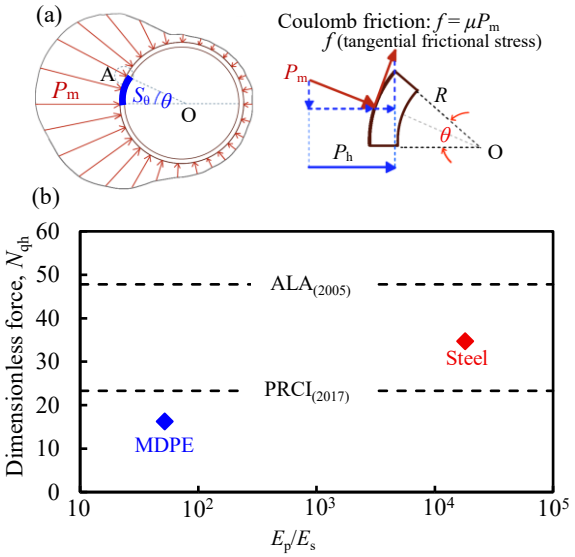

Figure 9. Normal pressure to force: (a) Sketch of pipe element with normal soil pressure, (b) N_{qh} from FE normal pressure with guidelines

The ALA (2005) guideline overpredicts the force for both pipe types, and more for the flexible MDPE pipe. The PRCI (2017) guideline provides lower forces for steel pipe and higher forces for MDPE pipe. More studies on the effect of pipe soil relative stiffness on the soil lateral load are currently underway and will be reported in future publications.

6 CONCLUSION

This paper presents an experimental and numerical study of steel and MDPE pipelines under lateral ground movement. The effects of pipe–soil relative stiffness on the lateral force on pipes are investigated. The experimental results were simulated using numerical models. The performance of MC and MMC models for analyzing different pipe behaviors was evaluated. Then, the maximum lateral soil force on the pipe was examined from the results of FE modeling. The study provides the following insights:

- The load transfer mechanism for buried pipes subjected to lateral ground movement varies based on the flexural rigidity of the pipes. This should be considered during interpretation of test results, particularly when presenting normalized forces.
- For the flexible MDPE pipe, the peak soil load mobilizes over a short length of the pipe towards the restrained ends, resulting in localized plastic deformation of soil. This does not affect the global load–displacement response, but it affects the local strain response of the pipe.
- The MMC model better simulated the strain softening behavior of the soil, while the MC model was inadequate. For the MDPE pipe, both the MC and MMC produced the same global response (i.e., load–displacement). However, only the MMC model successfully predicted the local strain measured during the tests.
- The dimensionless peak lateral force N_{qh} calculated from the FE analysis for the MDPE pipe is lower than that of the steel pipe. PRCI (2017) overestimates this force for MDPE and underestimates it for steel, while ALA (2005) recommendations overpredict the forces for both cases. The study suggests that the stiffness of the pipe should be considered when estimating maximum spring forces.

7 ACKNOWLEDGEMENT

The authors gratefully acknowledge the support provided by the Alliance Grants program of the National Science and Engineering Research Council of Canada, FortisBC Energy Inc., and SaskEnergy Canada Inc. for conducting this research.

8 REFERENCES

ALA (American Lifelines Alliance). 2005. Guidelines for the design of buried steel pipe, Reston, VA, USA: ASCE.

Almahakeri, M., Moore, I.D. and Fam, A., 2017. Numerical study of longitudinal bending in buried GFRP pipes subjected to lateral earth movements. *Journal of Pipeline Systems Engineering and Practice*, *8*(1), p.04016012.

Anzum, S., & Dhar, AS., 2023. Strain-softening effects of dense sand on lateral pipe-soil interaction. In Proc., 77th Canadian Geotechnical Conf., GeoMontreal.

Audibert, J.M. and Nyman, K.J., 1978. Soil restraint against horizontal motion of pipes. *Journal of the Geotechnical Engineering Division*, *103*(10), pp.1119-1142.

Choo, Y.W., Abdoun, T.H., O'Rourke, M.J. and Ha, D., 2007. *Remediation for buried pipeline systems under permanent ground deformation*. Soil Dynamics and Earthquake Engineering, 27(12), pp.1043–1055.

Dassault Systems. 2019. ABAQUS/CAE user's guide. Providence, RI: Dassault Systemes Simulia.

Jana Project, 2012. Engineering Assessment: Maximum Strain Criteria for PE Gas Pipeline, Technical report 12-1382, Jana laboratories, Ontario.

Janbu, N., 1963. Soil compressibility as determined by oedometer and triaxial tests. In *Proc. European Conf. SMFE, Wiesbaden, 1963* (Vol. 1, pp. 19-25).

Liu, J., Xie, Q., Ye, M., Ni, P. and Qin, X., 2023. Response of UPVC pipes buried in sand under lateral ground movement. *Tunnelling and Underground Space Technology*, *138*, p.105177.

O'Rourke, T.D., Jung, J.K. and Argyrou, C., 2016. Underground pipeline response to earthquake-induced ground deformation. *Soil Dynamics and Earthquake Engineering*, *91*, pp.272-283.

PRCI (Pipeline Research Council International), 2017. *Pipeline seismic design and assessment guideline*. Technical Report PR-268-134501-R01.

Roy, K., Hawlader, B., Kenny, S. and Moore, I., 2015. Finite element modeling of lateral pipeline–soil interactions in dense sand. *Canadian Geotechnical Journal*, 53(3), pp.490–504.

Suleiman, M.T. and Coree, B.J., 2004. Constitutive model for high density polyethylene material: Systematic approach. *Journal of Materials in Civil Engineering*, 16(6), pp.511–515.

Trautmann, C.H. and O'Rourke, T.D., 1985. Lateral force–displacement response of buried pipe. *Journal of Geotechnical Engineering*, 111(9), pp.1077–1092.

Xie, X., Symans, M.D., O'Rourke, M.J., Abdoun, T.H., O'Rourke, T.D., Palme, M.C. and Stewart, H.E., 2013. Numerical modeling of buried HDPE pipelines subjected to normal faulting: a case study. *Earthquake Spectra*, 29(2), pp.609–632.

Ye, M., Ni, P. and Maitra, S., 2024. Response of flexible pipes buried in sand under multi-directional movement: understanding fault-pipeline interaction. *Soil Dynamics and Earthquake Engineering*, *187*, p.108978.

Yang, H., Wang, L., Lei, Z., Dou, Y. and Guo, Z., 2024. Numerical investigation on uplift behavior for pipelines shallowly buried in sloping ground. *Computers and Geotechnics*, 167, p.106066.

Yimsiri, S., Soga, K., Yoshizaki, K., Dasari, G. and O'Rourke, T., 2004. Lateral and upward soil–pipeline interactions in sand for deep embedment conditions. *Journal of Geotechnical and Geoenvironmental Engineering*, 130(8), pp.830–842.